

BOX-BEHNKEN DESIGN-BASED DEVELOPMENT AND CHARACTERIZATION OF POLYMERIC FREEZE-DRIED NANOPARTICLES OF ISRADIPINE FOR IMPROVED ORAL BIOAVAILABILITY

DEBASHISH GHOSE^{1*} , CHINAM NIRANJAN PATRA¹ , SURYAKANTA SWAIN² , JAMMULA SRUTI¹

¹Department of Pharmaceutics, Roland Institute of Pharmaceutical Sciences, Berhampur-760010, Odisha, India. ²School of Pharmacy and Paramedical Sciences, K. K. University, Nalanda-803115, India

*Corresponding author: Debashish Ghose; *Email: dave.ghose87@gmail.com

Received: 02 Mar 2023, Revised and Accepted: 17 Apr 2023

ABSTRACT

Objective: This study aimed to develop and optimize isradipine-loaded polymeric freeze-dried nanoparticles prepared by solvent shifting method with the help of the experiment design for improving oral drug bioavailability and minimizing dosing intervals.

Methods: Isradipine is a potent anti-hypertensive drug that is matrixed in polymeric freeze-dried nanoparticles using solvent shifting. In this work, a 3-factor, 3-level box-Behnken design was used to optimize the process parameters like a drug: PLA concentration (A), poloxamer 407 concentration (B), and stirring speed (C). In addition, responses were measured as dependent variables such as percentage drug release, particle size (nm), Zeta potential (mV), and % entrapment efficiency.

Results: Mathematical equations and response surface plots were used to relate the dependent and independent variables. The optimization model exhibited 97.36 % drug release, 153.14 nm particle size, -25.9 mV Zeta potential, and 78.25% entrapment efficiency, respectively. The observed responses were in close agreement with the predicted values of the optimized process. Fourier transform infrared spectroscopy, morphological studies, and *in vitro* drug release studies characterized the prepared polymeric nanoparticles.

Conclusion: The improved freeze-dried polymeric nanoparticle samples exhibited an *in vitro* drug release rate of more than 90% at 24h. Based on *in vivo* pharmacokinetic parameters, the isradipine-loaded polymeric nanoparticles show better bioavailability than pure drug's suspension form.

Keywords: Isradipine, PLA, Quality by design, Critical quality attributes, Zeta potential, Pharmacokinetic parameters

© 2023 The Authors. Published by Innovare Academic Sciences Pvt Ltd. This is an open access article under the CC BY license (<https://creativecommons.org/licenses/by/4.0/>)
DOI: <https://dx.doi.org/10.22159/ijap.2023v15i4.47728>. Journal homepage: <https://innovareacademics.in/journals/index.php/ijap>

INTRODUCTION

The present era of nanotechnology has tremendous potential for solving the issues related to ineffective dissolution and diminished oral bioavailability of anti-hypertensive classes of drugs. Henceforth the applicability of the multiple drug delivery methods has come to light as the strategies for accelerating the development of novel drug molecules which are poorly soluble [1]. Thus, using the traditional dosage forms might lead to poor patient compliance and over-or under-medication [2]. Nanocarriers have garnered the attention of scientists lately, and they have exhibited significant advantages over traditional dosage forms in the oral delivery of hydrophobic drugs [3]. Polymeric nanoparticles have particle sizes ranging from 10 to 100 nm and are colloidal drug delivery vehicles. Biodegradable, synthetic, and natural polymers synthesize these nanostructures [4]. The curative effectiveness of polymeric nanoparticles is highly reliant on the release of drugs and polymeric biodegradation. Isradipine (ISRA), a dihydropyridine derivative classified as a calcium channel blocker, treats high blood pressure by blocking the effects of calcium ion transmembrane entry into smooth muscle cells in the vascular system. Due to its low oral bioavailability of (15-24%) (ISRA) faces the challenge of reduced therapeutic response and pharmacologic outcome, thus the present research was streamlined to develop and optimize a novel strategy by the implementation of a QbD (Quality by Design) approach. The method encompasses the design and development of PLA-based Isradipine-loaded lyophilized nanoparticles utilizing the technique of solvent displacement. Standard regulatory bodies like USFDA have authorized polymer PLA as a biocompatible and biodegradable copolymer of lactic acid [5]. PLA is a semicrystalline and amorphous linear aliphatic thermoplastic with clear clarity and attainable flexibility. As a result, we chose isradipine (ISRA), an extremely hydrophobic drug, for our research. Polymeric nanoparticles have sparked the interest of scientists in the last 20 y as a highly promising delivery system [6]. This method not only compensates for the errors in conventional optimization methods but also possesses added features, such as considering the correlation

between various influential elements with the possible outcome on critical attributes of quality (CQAs). The QTPPs identify critical quality attributes (CQAs) [7, 8]. The objective of this study was to develop and optimize isradipine-loaded polymeric freeze-dried nanoparticles prepared by solvent shifting method with the help of the design of experiment for the improvement of oral bioavailability and minimization of dosing intervals.

MATERIALS AND METHODS

Materials

Microlabs Pvt. Ltd provided isradipine, poloxamer 407, and (Poly-lactic acid) or polylactide (PLA) as a sample gift from Zyodus Cadila (Mumbai, India). Sigma Aldrich, India, provided acetone and mannitol. Throughout the study, all essential ingredients used in the research have been of excellent quality.

Methods

Preparation of PLA-based nanoparticles

To synthesize these nanoparticles, the authors had to use a solvent-shifting strategy. The organic phase consisted of 10 ml of acetone, which dissolved the required quantities of isradipine and PLA. The stabilizer concentrations of (0.5% w/v, 1.0% w/v, and 1.5 % w/v poloxamer 407) were added to the aqueous phase, which was then added and mixed with the organic phase steadily through an injection syringe of gauge size # 27, this set up was subjected to 1h of continuous magnetic stirring (Model: Remi 2MLH) at 2000 rpm, to eliminate the unwanted residues of acetone the formulation was subjected to rotary evaporation technique (Model: Blue RV 10 Digital V-C Rotary Evaporator). After that, it was subjected to ultrasonication (Model: SONIC and MATERIAL VCX-500) for about 10 min at a 40% amplitude ratio to promote uniformity and the reduction in the size of the particles. The prepared nanosuspension was then filtered before lyophilization (Model: Martin Christ Alpha 2LD PLUS) by adding a cryoprotective agent (PVP) 5% at -58 °C and 0.040 pressure. These freeze-dried formulations were transferred

carefully into the glass vials and kept in a desiccator for future research findings and characterizations [9].

Critical quality characteristics (CQAs) and quality target product profiles (QTPPs)

In a broad sense, QTPP is a prerequisite for creating the necessary quality in terms of safety and efficacy, as well as facilitating the diagnosis of product CQAs [10]. The QTPPs were determined based on regulatory, scientific, and practical factors and risk assessments, as stated in table 1. CQAs are established utilizing QTPPs, which manage the creation of processes and products [11, 12].

Table 1: Estimated parameters with the pre-determined target for PLA-loaded ISRA nanoparticles

Quality target product profiles (QTPPs)	Target	CQAs	Pre-determined target	Justification
Dosage type	Sustained release dosage forms	% Drug release at 24h	≥ 90-95%	The study's objective is to accomplish sustained drug release, which is essential for greater absorption.
Dosage form	Freezed dried nanoparticles	Zeta potential	≥±20mV	In terms of nanosuspension stability, this is one of the critical factors.
Drug release and absorption	Cmax and AUC higher compared to pure drug	Mean particle size (nm)	100 nm-200 nm	Particle size in these ranges is incredibly important and essential for drug solubility and absorption.
Enhanced entrapment	Higher entrapment	Entrapment efficiency	65-80%	Higher entrapment efficiency is essential for drug dose management and therapeutic efficacy, thus being extremely essential.

Analytical method based on ultra-fast liquid chromatography (UFLC)

The methodology was facilitated using an ODS C18 (250 mm x 4.6 mm x 5 mm) chromatographic column and a (Model: Shimadzu SPD-20M) liquid chromatographic system with a photodiode array (PDA) detector. The final optimized trail was acquired using acetonitrile and water (70:30%v/v) as the solvent system (mobile phase), a flow rate of 1 ml/min, and a run time of 5 min. With a column oven temperature of 40 °C, the injection volume was kept consistent at 20 µl. Chromatographic identification was carried out by employing a PDA detector with a maximal wavelength of 254 nm. Furthermore, with a retention time (Rt) of 4.821 min and no peak interference, this novel method is efficient for the drug isradipine [17].

Preliminary screening by taguchi orthogonal array (OA design)

A preliminary assessment was conducted using a Taguchi design with seven components and two levels to identify the most relevant factor(s) impeding the CQAs. An array of eight formulations for Taguchi design of the experiment matrix were developed and built, accompanied by evaluation for the CQAs presented. An ANOVA was applied to assess the overall significance of each aspect. Finally, the p-value was actualized to identify the essential factors [18].

Systematized optimization of formulation by the design of experiments (DoE)

A 3-factor, and 3-level Box-Behken Design response surface method was utilized to optimize the composition of polymeric nanoparticles. The experimental trials were developed using Stat-Ease Design Expert ver. 12.1.1 software, with the ratio of Drug: PLA (mg) (X1) and Poloxamer 407 % w/v (X2), Stirring speed(X3) as independent variables, and three levels (-1, 0, and 1) generated to examine the substantial effect of these numerous elements or response. Precisely, % drug release (Y1), particle size in nm (Y2), zeta potential mV (Y3), and % entrapment efficiency (Y4). After assembling the 17 formulation runs, CQAs were checked [19].

Solid-state characterization methods

Micromeritic method

The flow properties (angle of repose), % moisture content, and Carr's index of the developed freeze-dried PNs of ISRA were evaluated to understand the content uniformity, feasibility, and scalability aspects of these powders in the subsequent dosage forms [20, 21].

Measurement of particle size and zeta potential

The particle size was determined using the Malvern apparatus of (Model: Malvern ZETASIZER NANO ZS Malvern ZEN3600 RED) laden

Screening of solvents based on solubility

To investigate the drug's solubility, acetone, ethanol, DMSO, distilled water, phosphate buffer 6.8 and 7.4, 0.1N HCl, methanol, acetonitrile, DMF, PEG 200, and 400 were all utilized. A reasonable quantity of the drug was incorporated into each solvent. The solution was agitated for 72 h in a mechanical shaker (Rivotek, Riviera Glass Pvt. Ltd.) with a temperature condition maintained at 37±0.5 °C within a water bath. The vials were examined for complete solubilization of the drug substance frequently. All mixtures were allowed to be inserted into centrifuge tubes in order to eliminate any insoluble or immiscible drugs [13-16].

with (PCS) that was implied to estimate and assess the particle size and zeta potential. The uniformity within the colloidal dispersion is highly influenced by zeta potential values [22].

Estimation of entrapment efficiency

The % entrapment efficiency of the drug ISRA within the fabricated polymeric nanoparticles was determined by measuring the concentration of (ISRA) within these nanostructures. The estimation was carried out by taking 10 ml of ISRA PNs, which were subjected to centrifugation by a cooling centrifuge (Model: Eltec Lab RC 4815) for a period of 30 min at a temperature of -4 °C at 10000 rpm. The centrifugation dialysis process helps remove the untrapped free drug [23]. The drug entrapment efficiency (%EE) of these PNs of ISRA was determined and calculated, as shown in Eq. (1)

$$\% \text{ Entrapment Efficiency} = \frac{\text{Total drug quantity} - \text{Quantity of free drug}}{\text{quantity of total drug}} \times 100 \dots [\text{Eq. 1}]$$

Fourier transform infrared spectroscopy (FT-IR)

The physical interactions of the drug isradipine were identified via FT-IR spectrometry (Model: SHIMADZU IR AFFINITY-1). FT-IR spectrum of varied isradipine and physical combinations (PM) with PLA and poloxamer 407 was generated utilizing Potassium bromide. The drug-excipient interaction was evaluated using calculated transmittance from 4000 to 400 cm⁻¹. Peak matching was used to assess any interactions between isradipine and the additional excipients [24].

Differential scanning calorimetry (DSC)

DSC (Model: SHIMADZU DSC-60) evaluation was utilized to explore the drug's compatibility with the polymer. Dried nitrogen was applied as the effluent gas to warm all specimens (10 mg) in aluminum pans. DSC thermograms of isradipine, PLA, and Poloxamer 407 and physical combinations of ISRA and PLA, ISRA and poloxamer 407 were determined [25].

In vitro drug release

In this *in vitro* drug release analysis for pure drug ISRA, the dialysis bag diffusion approach (Himedia; dialysis membrane-60; Avg. flat width-25.27 mm, Avg. diameter-15.9 mm with 10000 kDa-12000kDa with 5 ml capacity) was used. For the initial 2 h, 5 ml of all formulations were loaded in a dialysis membrane, sealed, and dipped in 150 ml of 0.1N HCl at sink conditions. It was then immersed in a 6.8 pH phosphate buffer solution for 24 h. The system was maintained at 37 °C with constant magnetic stirring at 200 rpm. Next, samples (2 ml) were removed from the receptor compartment at preset time intervals and replaced with fresh 0.1 N HCl and

phosphate buffer pH 6.8. After that, 1 ml of ethyl acetate was added to the sample and separated into 1 ml. The solutions were vortexed in a cyclomixer, and the supernatant layer was collected in a test tube containing 0.5 ml. This test tube was preserved for drying before injecting the mobile phase and examining it with RP-UFLC [26, 27].

Pharmacokinetic studies *in vivo*

The pharmacokinetic profile parameters of isradipine in rabbit serum after an oral dose of 0.46 mg of isradipine nano-formulation and 0.93 mg of pure drug in suspension form were evaluated that used a rapid and effectively validated RP-UFLC methodology. 12 male albino rabbits weighing 2 kg were selected. They were divided into two groups of six animals each, one for the test (nano-formulation) and one for the standard (control) (aqueous suspension of isradipine). They were also served sterile meals and given fresh water twice a day. Before testing, all animals were subjected to a 15-day washout period [28]. On the contrary side, the test proved accurate and sensitive enough to predict isradipine concentrations in rabbit serum samples. Nevertheless, the test proved robust and adequately sensitive to identify isradipine on a consistent basis.

The dose for rabbit was calculated as follows

$$\begin{aligned} \text{Total dose (in humans)} &\times 0.07(\text{factor for each rabbit}) \times 2\text{kg weight of rabbit} / 1.5 \\ &= \frac{5\text{mg} \times 0.07 \times 2}{1.5} = 0.46\text{mg} \dots (\text{Eq 2}) \end{aligned}$$

Collection of blood samples and study design

Animals have fasted for a single-dosage bioavailability study. The oral bioavailability of the enhanced ISRA composition and an aqueous suspension of the pure drug was examined in rabbits [29]. For the research, a healthy breed of male rabbits was taken. Then, 1 ml of blood was collected from the animal's ear vein as a blank sample. The animal was then given a pure medication solution in distilled water. Blood was collected from both rabbits' ear veins at 2h intervals (0, 2, 4, 6, 8, 12, and 24h) at different time points. After that, the samples were then centrifuged for 20 min at 5000 rpm. The serum (supernatant layer) was carefully collected using a micropipette. The UFLC technique was used to examine all of the samples. The area under the curve (AUC) and many pharmacokinetic parameters were calculated, including the elimination rate constant (K), half-life ($t_{1/2}$), peak plasma concentration (C_{max}), time to obtain peak plasma concentration (T_{max}), and peak plasma

concentration (C_{max}). Additionally, the pharmacokinetic investigation was authorized by the Institutional Animals Ethics (926/PO/Re/5/06/CPCSEA, Approval No. 105), of Roland Institute of Pharmaceutical Sciences, Berhampur. All animal tests were carried out following the ARRIVE recommendations and in conjunction with the UK Animals (Scientific Procedures) Act, 1986 and related guidelines, as well as EU Directive 2010/63/EU on animal research.

Powder X-ray diffraction (p-XRD)

A powder X-ray diffractometer was used for the diffraction investigations (Model: Rigaku, Japan, Smart Lab 9 kW). The samples were subjected to nickel-filtered CuK α radiation (40 kV, 30 mA) and scanned to undertake powder-XRD. It was carried out on ISRA's pure drug and optimized lyophilized PNs. After that, the results were plotted as peak height (intensity) versus time (h) [30].

Scanning electron microscopy (SEM)

The morphology of nanoparticles has been examined using high-resolution, 30 kV scanning electron microscopy (Model: Jeol, JSM-6390LV) Japan. Initially, the formulation sample adhered to the carbon-coated metallic stub. However, since it utilizes a high-energy electron to scan over the surface of a specimen with an Au and Pt coating to improve contrast and signal-to-noise ratio [31], SEM helps to explore surface characteristics in depth. In addition, ISRA's pure drug and optimized lyophilized PNs were evaluated, and surface morphology was assessed.

Accelerated stability study

The improved nanoparticle formulation was tested for 6 mo in a stability chamber (Model: TH 200G, Thermolab, Thane, India). The formulations were packed in capsules and packed in a glass container with a cotton seal until they were kept at 40 °C in a stability chamber. After 0, 1, 2, 3, and 6 mo of stability, the specimens were assessed for particle size, zeta potential, and drug release.

RESULTS

Screening of solvents on the basis of solubility

In acetone, DMSO, and ethanol, the saturation solubility of isradipine (ISRA) was 3026.33±115.22 µg/ml, 2458.22±102.40µg/ml, and 4365.22±109.34 µg/ml, as illustrated in fig. 1 respectively.

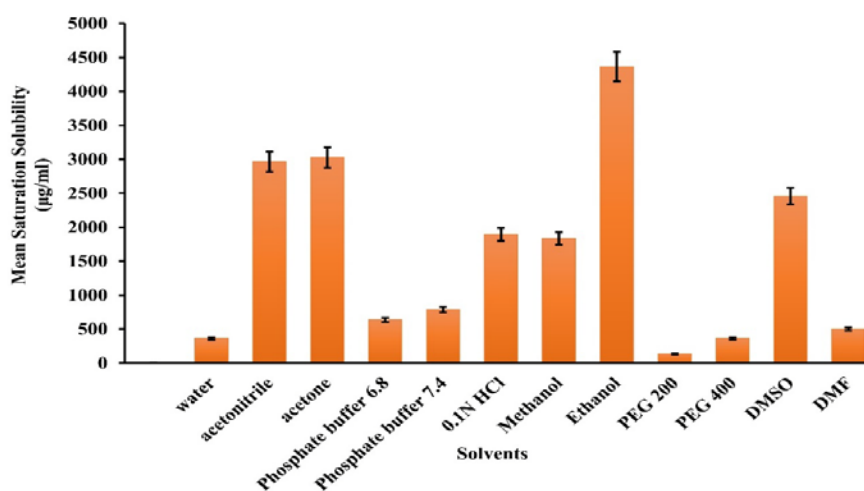


Fig. 1: Saturation solubility for selection of solvent, all data showed as mean±SD (n=6); where n is the number of observations

Taguchi-based design for factors screening

The Taguchi screening was conducted based on the selection of the different factors as suggested by the design matrix along with their coded values, such as A-Drug: PLA concentration and B-Poloxamer

407 concentration, C-Ultrasonication time, D-Stirring speed, E-Stirring type, F-Temperature, and G-Stirring time, as depicted in table 2. The relationship between the individual factors and their causative effect on each response are correlated using the *p*-values of the regression coefficients.

Table 2: Design matrix for factor screening as per taguchi design along with the experimental results of various CQAs

Runs	A	B	C	D	E	F	G	% Drug release	Particle size (nm)	Zeta potential (mV)	Entrapment efficiency
1	1	2	2	1	1	2	2	66.85	259.45	-9.5	0.452
2		2	2	1	2	1	1	39.23	435.46	-4.1	0.562
3		2	1	2	1	2	1	47.45	365.36	-5.4	0.541
4		1	1	1	2	2	2	82.33	210.36	-19.3	0.366
5		2	1	2	2	1	2	50.36	315.23	-6.5	0.531
6		1	1	1	1	1	1	79.58	232.56	-12.5	0.399
7		2	2	1	1	2	2	40.23	385.22	-4.2	0.671
8		1	2	2	2	1	1	58.34	295.47	-7.5	0.481
Factors				Codes				Low level (1)	High level (2)		
PLA conc.(mg)				A				5	10		
Poloxamer 407 conc (gm%)				B				1%	2%		
Ultrasonication time (mins)				C				5	15		
Stirring speed(rpm)				D				1000	2000		
Stirring type				E				Magnetic	Mechanical		
Temperature ° C				F				25	40		
Stirring time (h)				G				1	2		

Design, optimization, and analysis of experiments

Table 3. Depicts the systematized combinations of all 17 formulations as per the box-Behnken design. It consisted of 3-factor 3-level design matrix that was further utilized to study the effect of influential factors such as Drug: PLA concentration, poloxamer 407

concentration and Stirring speed upon the observed responses. Each component consisted of three levels (-1, 0, and 1) low, intermediate and high levels of the factors which were selected through the preliminary screening methods and its data analysis from the Pareto-charts. All the 17 formulations were further characterized to determine the effects of multiple parameters on individual CQAs.

Table 3: Composition of optimized runs of polymeric nanoparticles (ISRA) as per box-Behnken design with stated CQAs

Runs	Factor 1 A: Drug: PLA conc	Factor 2 B: Poloxamer 407 conc	Factor 3 C: Stirring speed	Response 1 Drug release	Response 2 Particle size	Response 3 Zeta potential	Response 4 Entrapment efficiency	
	mg	gm%	rpm	%	nm	mV	%	
1	1	1	0	12.22	652.11	-5.65	13.25	
2	0	0	0	72.29	235.89	-21.89	65.69	
3	1	0	-1	19.36	593.35	-7.5	20.01	
4	0	0	0	66.25	269.21	-21.64	60.91	
5	0	1	1	52.09	273.69	-20.26	58.12	
6	0	0	0	60.45	290.11	-20.01	55.22	
7	0	1	-1	49.87	329.65	-17.33	40.1	
8	0	0	0	59.15	301.96	-19.67	49.78	
9	0	-1	1	40.89	378.11	-16.47	35.98	
10	-1	0	1	76.18	210.25	-22.36	70.66	
11	1	-1	0	33.59	510.45	-11.66	26.11	
12	-1	0	-1	39.58	432.09	-14.55	32.62	
13	-1	1	0	97.36	153.14	-25.9	78.25	
14	0	0	0	55.36	316.21	-18.11	44.22	
15	-1	-1	0	80.26	190.44	-22.95	73.55	
16	1	0	1	26.55	529.15	-10.22	24.54	
17	0	-1	-1	34.56	493.32	-12.64	29.66	
Independent variables				Levels				
X1: DRUG: PLA ratio (mg)				Low (-1)		Medium (0)		High (1)
X2: POLAXOMER 407 CONC %				1:1(5 mg)		1: 1.5 (7.5 mg)		1:2(10 mg)
X3: STIRRING SPEED (rpm)				0.5%		1%		1.5%
				1000		1500		2000

2D and 3D response surface analysis

Effect of the factors on % drug release, particle size, zeta potential and entrapment efficiency as CQAs

The CQA % Drug release contour plot and 3D plot are shown in fig. 2(a) and 2(b). Trial run No.13 seemed to have the highest percentage of release, 97.36 %, as shown in a comparison among these formulations. Run No. 1 has a minimal value of 12.22% due to high levels (1) of Drug: PLA concentration and the high level of Poloxamer 407 concentrations, which may be attributable to the greater concentration of polymer PLA resulting in enhanced particle size and reduced drug diffusion. The contour plot and 3D plot of the CQA particle size are depicted in fig. 2(c) and 2(d). It varies from 153.14 nm for run 13 to 652.11 nm for run 1. The contour plot and

the 3D plot of the CQA zeta potential are depicted in fig. 2I and 2(f). Both the concentrations of A-Drug: PLA and B-Poloxamer 407 appear to significantly impact the CQA Zeta values. At a lower level, it varies from -25.9mV for run 13 to -5.65mV for run 1. The contour plot and the 3D plot of the CQA %entrapment efficiency are shown in fig. 2(g) and 2(h). The % Entrapment appears to be influenced equally by A-DRUG: PLA and B-Poloxamer 407 concentrations. It ranges from 78.25% for run 13 and 13.25% for run 1.

ANOVA of the experimental design

The ANOVA summation for multiple elements and their relevance in regard to the quadratic model was identified. The model F-values for drug release, particle size, zeta potential, and entrapment efficiency were reported to be 8.79, 10.35, 9.61, and 5.43, respectively. *p*-values

for the quadratic model for distinct CQAs are less than 0.05, implying that the model has statistical significance. Its *p*-values for % drug release, particle size, zeta potential and % entrapment efficiency were estimated as 0.0061, 0.0387, 0.060, and 0.0238, respectively, and *p*-values less than 0.05 indicate that the model terms are substantial. The perturbation and the predicted v/s actual plots for the observed values are effectively illustrated in fig. 3 (A-H).

Analyses overlay plots to establish the design space

The optimized ISRA PNs were produced utilizing the Box-Behnken design with 5 mg ISRA, 5 mg PLA, and 1% w/v Poloxamer-407 concentrations. Table 4 shows an overview of the optimization

approach as well as the predicted and experimental values of the optimized formulation's responses.

Solid-state characterization of PNs

Micromeritic investigations

The angle of repose is 29.92±0.36°, the percent moisture content is 2.3±0.6, and the Carr's index is 15.24±0.94, according to the micromeritic characteristics of lyophilized polymeric nanoparticles as depicted in table 5. Run 13 was identified as the best formulation with improved flow properties based on these micromeritic parameters.

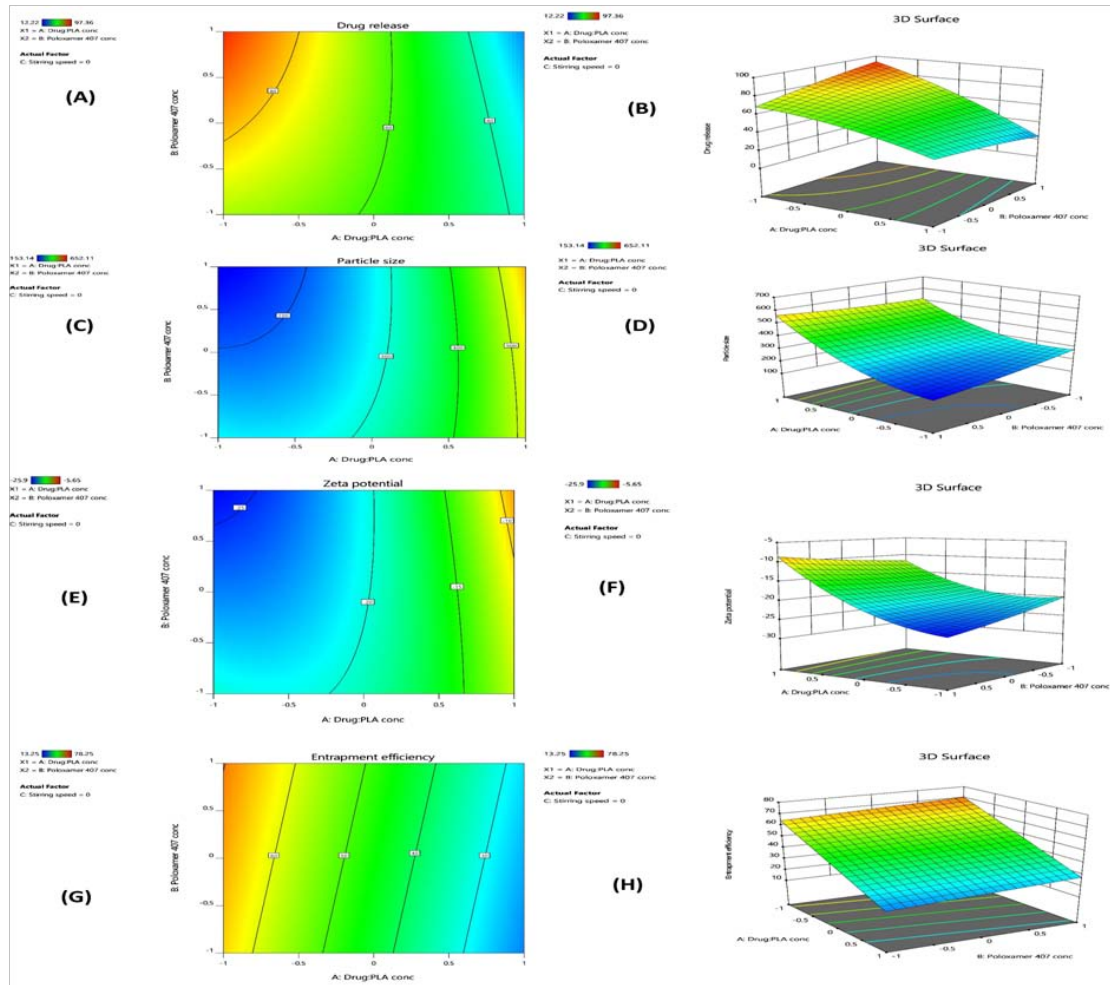


Fig. 2: (A) and (B) % Drug release, (C) and (D) particle size, (E) and (F) zeta potential and (G) and (H) % Entrapment efficiency for the (2D) and (3D) plots of the chosen influential factors on observed CQAs

Table 4: Illustrates the predicted and observed response values for the CQAs

Run 13 response	Predicted mean	Predicted median	Observed	Std dev	SE mean	95% CI low for mean	95% CI high for mean	95% TI low for 99% pop	95% TI high for 99% pop
Drug release (%)	93.46	93.46	97.36	11.52	9.98	69.86	117.06	21.20	165.71
Particle size (nm)	148.93	148.93	153.14	72.95	63.18	-0.47	298.34	-308.51	606.38
Zeta potential (mV)	-25.79	-25.79	-25.90	2.59	2.24	-31.10	-20.48	-42.05	-9.53
Entrapment efficiency (%)	70.25	70.25	78.25	12.87	7.15	54.79	85.709	8.32	132.18

Particle size and zeta potential measurement

The optimal size range for ISRA's PNs was discovered to be (153.14 nm), i.e., for run 13. Depicted in fig. 4(a). The Isradipine loaded PLA-

NPs produced were spherical, with a homogeneous size distribution and particle size of 200 nm.

Run No. 13 had a zeta potential of (-25.9) fig. 4(b).

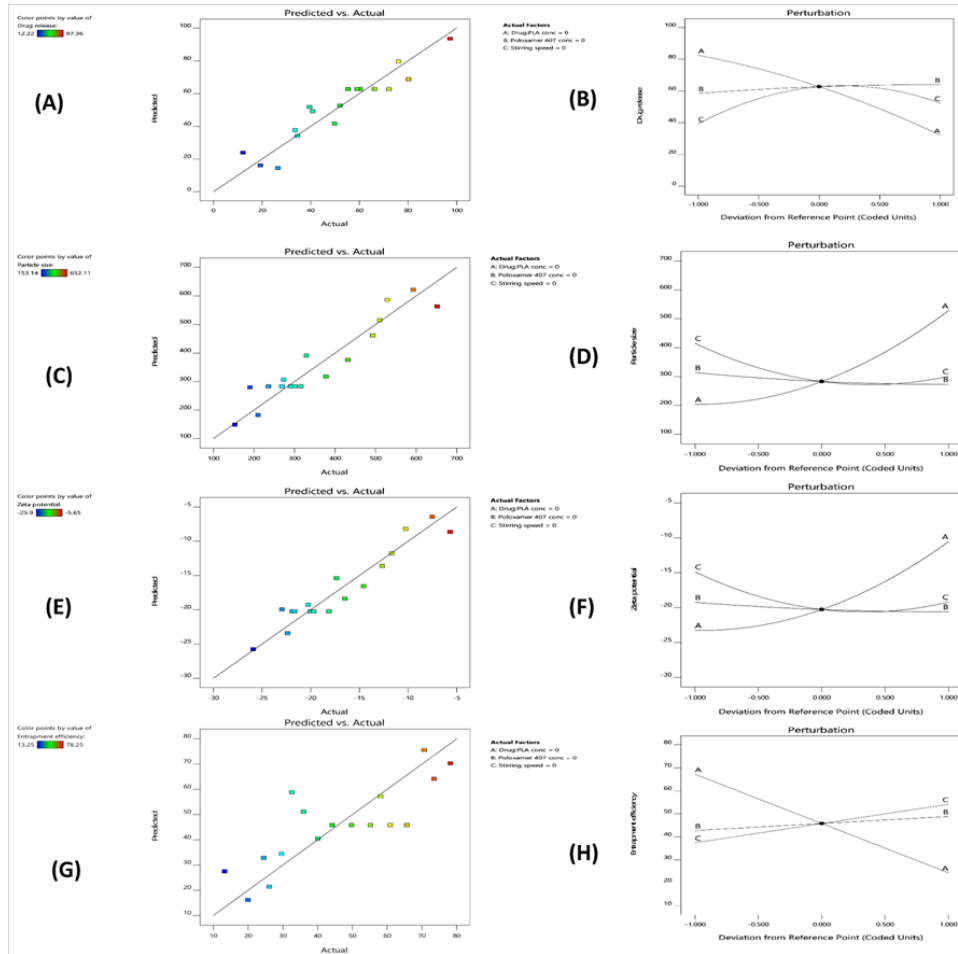


Fig. 3: (A) and (B) %Drug release, (C) and(D) particle size, I and (F) zeta potential and (G)and(H) % Entrapment efficiency for the predicted v/s actual plots and perturbation plots of the observed responses

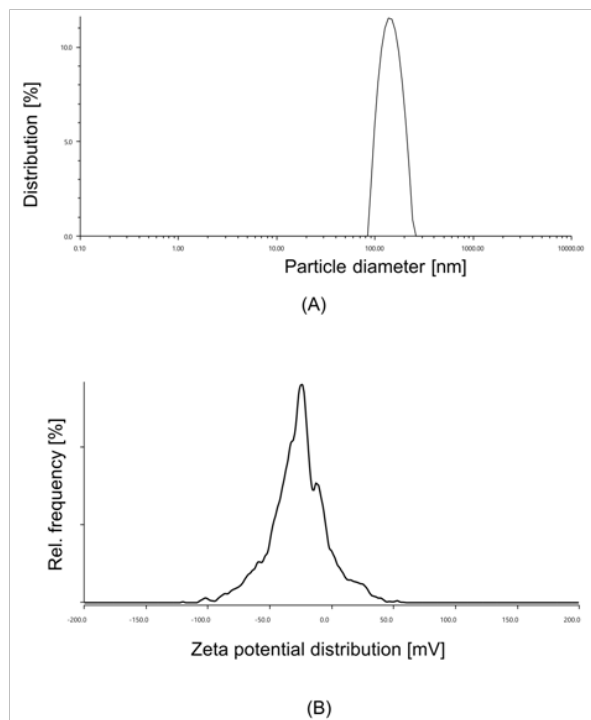


Fig. 4: (A) Particle size distribution and (B) zeta potential curves of optimized formulation batch

Table 5: Micromeritic parameters and % moisture content of the pure isradipine and polymeric formulation (optimized)

Formulations	Carr's index	Angle of repose (θ)	Moisture content (%)
Pure drug ISRA	26.59±1.08	37.5±1.22	2.9±0.54
Optimized formulation	15.24±0.94	29.92±0.36	2.3±0.6

All data showed as mean±SD (n=6); where n is the number of observations

Entrapment efficiency

Of all 17 experiments conducted, Poloxamer-407 1.5% w/v at a stirring speed of 1500rpm was reported to have the maximum entrapment efficiency (78.25%) (Drug: PLA concentration 5:5 mg).

Fourier transform infrared spectroscopy (FT-IR)

The interactions between isradipine and polymer were investigated using FT-IR spectroscopy. FT-IR spectra of selected ISRA and physical mixture (PM) with PLA and Poloxamer 407 were recorded on IR employing Potassium bromide with a resolution of 4 cm⁻¹ in the 4000-400 cm⁻¹ range. In FT-IR investigation for purified isradipine, C-N stretching at 1224 cm⁻¹, C-O vibration at 1669 cm⁻¹, N-H at 3694 cm⁻¹, O-H vibration at 3624 cm⁻¹, and C=C vibration at

3244 cm⁻¹ were identified. Finally, as shown in FT-IR studies of a combined effect of polymers and drugs, there is no significant change as depicted in fig. 5(A-E).

Differential scanning calorimetry (DSC)

The thermograms of isradipine(ISRA) reveals a prominent peak at 169.11 °C, revealing the drug's crystalline nature, an onset temp of 165.69 °C, and an end set temp of 172.42 °C, that correlates to the drug's melting temperature. ISRA DSC thermograms and physical ISRA mixtures with adjuvants have been examined. The thermograms of ISRA displayed a strong endothermic peak at 169.11 °C (Tfus), with a latent heat of fusion (Hfus) of-39.28mJ, as shown in fig. 6(a-e).

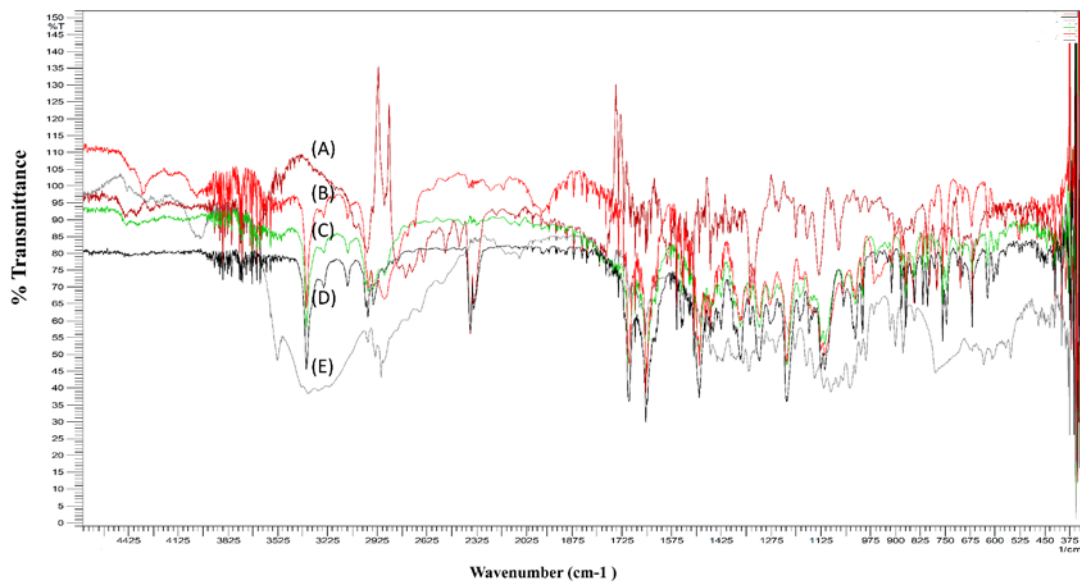


Fig. 5: FT-IR spectrum of (A) pure drug, (B) Poloxamer 407, (C) PLA, (D) Drug+polymer mixture (E) Formulated PLA-loaded nanoparticles

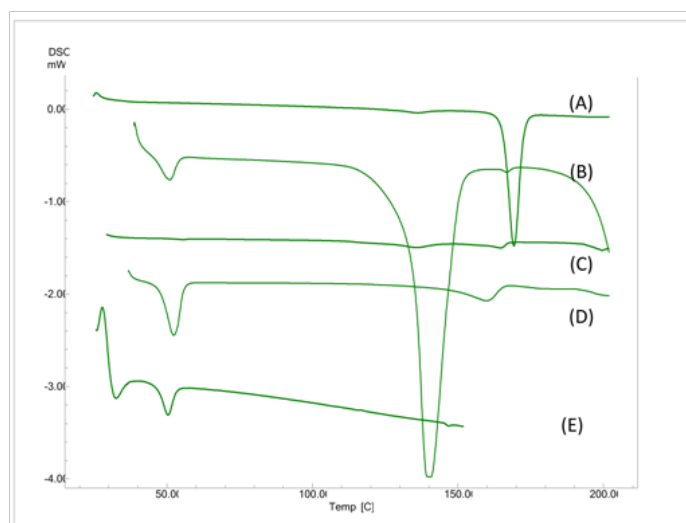


Fig. 6: DSC thermogram of (A) pure drug, (B) Poloxamer 407, (C) PLA, (D) Drug+polymer mixture (E) Formulated PLA-loaded nanoparticles

Studies on drug release *in vitro*

Fig. 7(a) illustrates the drug release behaviour for ISRA and pure-drug optimised PNs. The graph demonstrated that the optimised batch had a significant increase in drug release of about 97.36% at 8h, i.e. over 1.5 times more drug release than the pure drug following an 8h study. The optimal drug-loaded PNs R² values were determined to be 0.889,

0.833, and 0.958 for pure drug, 0.978 for zero-order, 0.952 for first-order, and 0.922 for the Higuchi model. The formulations (F13, F15 and F10) exhibited better drug release due to the presence of lower proportion of Drug: polymer (PLA) concentration, whereas an exception was observed with the formulation (F12); with a prevalence of diminished drug release of (39.5%) at 24h, which could be attributed to its lower stirring speed during the process i.e., 1000rpm.

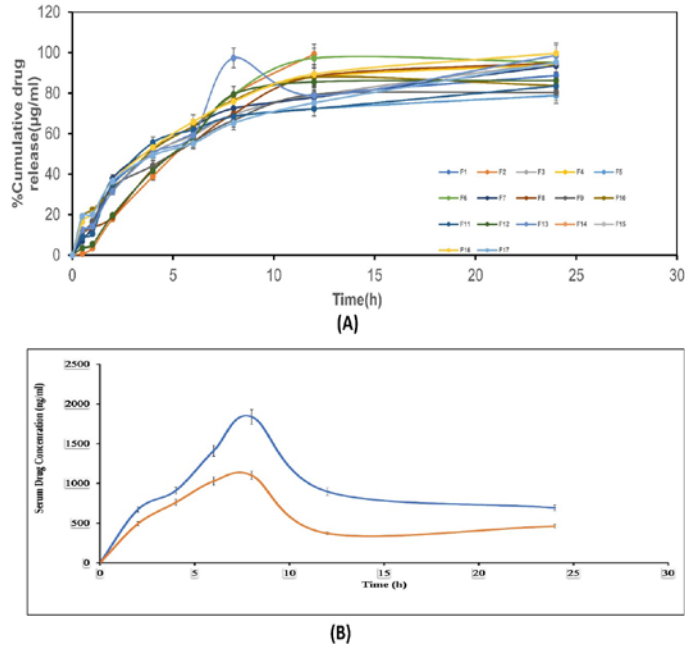


Fig. 7: (A) *In vitro* drug release of the prepared formulations, (B) Serum-drug concentration (ng/ml) v/s time (h) curve of optimized formulation batch vs pure drug suspension. All data showed as mean±SD (n=6); where n is the number of observations

Pharmacokinetic *in vivo* study

Fig. 7(B) illustrates its mean plasma levels of ISRA vs. time plots of the optimized PNs of ISRA and pure drug after the pharmacokinetic investigation. These estimated parameters for several pharmacokinetic parameters are reported in table 6. T_{max} was observed to be 8h for the

improved formulation, compared to 8h for pure-drug ISRA, showing that the drug was released consistently. The amplified ISRA PNs had a C_{max} of 1836.55ng/ml, in comparison to 822.69ng/ml for the pure ISRA drug. The AUC of optimized ISRA PNs was observed to be 28936.63 (ng/h/ml), which is more than three-fold greater than that of the area under the curve of the pure drug (9457.25 (ng/h/ml)).

Table 6: Pharmacokinetic values (*In vivo*) of isradipine (pure drug suspension) and improved polymeric nanoparticles

Formulations	C _{max} (ng/ml)	T _{max} (h)	K _e	AUC _{∞ 0} , (ng/h)/ml
Isradipine suspension (drug)	822.69±0.025	8±0.062	170.5	9457.25±0.056
Optimized formulation	1836.55±0.011	8±0.021	182.7	28936.63±0.048

All data showed as mean±SD (n=6); where n is the number of observations, except K_e

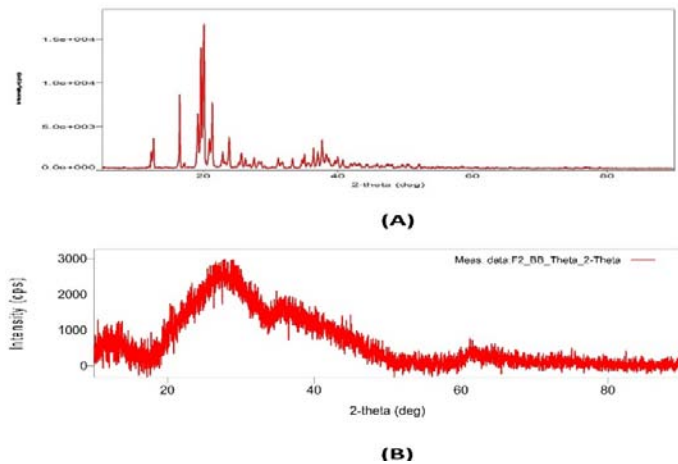


Fig. 8: P-XRD graphs of (A) Isradipine (pure drug), (B) freeze-dried polymeric nanoparticles

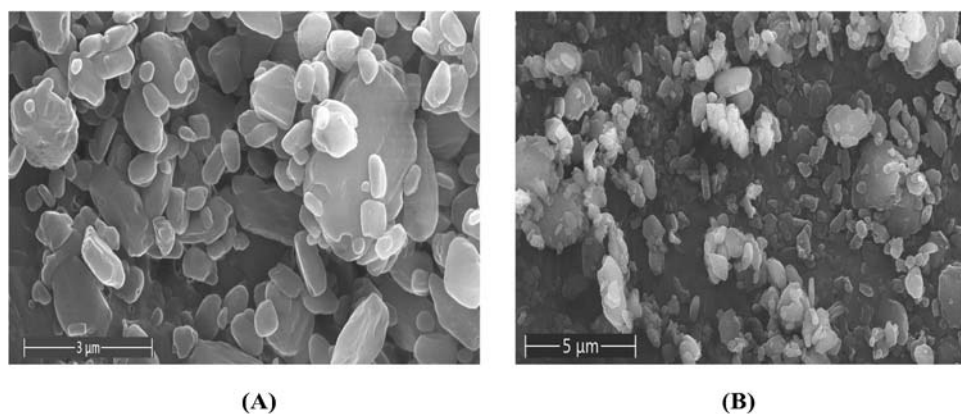


Fig. 9: Illustration of SEM (A) Isradipine (pure drug), (B) Freeze-dried polymeric nanoparticles

Table 7: Post-accelerated stability values of the CQAs (%drug release, particle size, zeta potential and %entrapment efficiency

Time in (Months)	% Drug release	Particle size (nm)	Zeta potential (mV)	% Entrapment efficiency
0	97.369±0.02*	153.14±0.01*	-25.9±0.03*	78.25±0.02*
1	93.332±0.06*	156.32±0.02*	-26.36±0.04*	72.30±0.03*
2	91.258±0.12*	159.22±0.06*	-28.28±0.01*	70.25±0.05*
3	89.560±0.22*	164.10±0.01*	-28.69±0.02*	68.35±0.04*
6	83.223±0.03*	164.96±0.02*	-29.21±0.06*	64.06±0.02*
<i>p</i> -value $\alpha \leq (0.05)$ significant difference exists	0.077	0.069	0.085	0.065

(*) % Drug release, Particle size, Zeta potential and % Entrapment efficiency are represented as mean±SD (n=6); where n is the number of observations

Powder X-ray diffraction (p-XRD)

Fig. 8(A) and 8(B) exhibit the XRD patterns of pure drug ISRA and optimum ISRA PNs. Pure-drug ISRA diffraction angles of 15.9°, 17.3°, 18.9°, 20.1°, 20.4°, 23.6°, and 24.2° exhibited significant peaks, affirming a typical crystalline pattern.

Scanning electron microscopy (SEM)

The SEM pictures of isradipine (pure drug) and optimum PNs of ISRA are shown in fig. 9(A) and (B), correspondingly.

Accelerated stability studies

The table 7 shows the ANOVA design's *p*-values during the accelerated stability study. The *p*-value for all CQAs is more than 0.05, suggesting no significant change.

DISCUSSION

The selection of solvents was based on the drug's peak solubility (i.e., quantitative solubility for other co-solvents) among the various solvents, such as ethanol, acetonitrile, methanol, phosphate buffer pH 6.8, and pH 7.4 and DMSO was determined. Still, acetone has been selected as a solvent for the required study based on the solubility, which was found to be maximum compared to other solvents. Taguchi Orthogonal array design was undertaken to predict the influential factors with numerous trials for each aspect during the preliminary screening of the influential factors; out of all seven significant parameters, only three highly critical ones were selected and justified as per the CQAs. The influential variables like the Drug: PLA concentration, the Poloxamer 407 (%w/v) stabilizer concentration, and the stirring speed were highly significant variables that were further considered for the design optimization and identification of design space within the predicted range. Similar results were also reported by Alam T, Khan S, *et al.* in 2018.

Effect of the factors on %drug release as CQAs: This was suggested by the reddish zone from the 2D and 3D plots, which is anticipated to be predominant at a low level (-1) of Drug and PLA ratio and a higher level (1) of stabilizer, i.e., Poloxamer 407 (%w/v), signifying greater than 90% release of drug in 24h, based on the simulations. The particle size and aggregation increased with the elevation in the polymer concentration, which was noticed in other trials with higher

levels (1) of the Drug: PLA ratio. Thus, this prolonged the release process and significantly influenced the dissolution performance [32].

Effect of the factor on Particle size as CQAs: The low level of factors A-Drug: PLA concentration (-1), it was also observed that a bluish tinge region persisted, i.e., the existence of lesser particle size, which is shown by drug-polymer concentration at (-1) and high level (1) of stabilizer. Therefore, it can also be anticipated that at low levels of A-Drug: PLA concentration, particle size is diminished, and this lowers dramatically as the factor A-concentration rises, as indicated by the light yellowish zone [33], and an increase in PLA concentration leads to an increase in viscous forces that resist droplet disintegration by stirring and sonication.

Effect of the factor on ZP as CQAs suggested the prevalence of dark blue area, which promises to have a substantial impact on the above CQA [34], it implies a higher value of zeta potential for A-Drug: PLA concentration low level (-1) and B-Poloxamer 407 concentration at a high level (1).

Effect of the factor on %entrapment efficiency as CQAs and its findings revealed that the %EE value remains below 80% when the polymer and stabilizer ratio is within the (-1 to 1) coded range. The stabilizer concentration plays a vital role appropriate entrapment of the drug within the polymeric nanostructures [35].

The micrometric characteristics of lyophilized polymeric nanoparticles suggested that particles exhibited good flow properties and the percentage moisture content within the desired range. Therefore, these lyophilized powders should exhibit a desirable flowability and compressibility for their further scale-up and processing into tablet and capsule dosage form.

The zeta-sizer device was employed to assess the size of the particles of all compositions. A few formulations had particle sizes more prominent than 500 μm, implying that polymeric nanoparticles were less likely to be present. In addition, the increasing polymer content had a pleiotropic effect on the size of particles, producing a hazy aspect because of higher aggregation.

The effect of various process factors demonstrates that the solvents, excipients, and method were adopted appropriately. Inadequate entrapment causes the PNs to rupture, which reduces the drug

loading and entrapment efficiency of all PNs manufactured with different stabilizer concentrations. Thus, the optimized formulation showed enhanced entrapment efficiency.

The interactions between isradipine and polymeric mixtures were studied using FT-IR analysis. The FT-IR spectrum of specified Isradipine and physical mixtures (PM) with PLA and Poloxamer 407 were analyzed. Because these peaks remained intact in the IR spectra of the physical mixtures, this shows no interactions between the drug and the polymers. The result indicated Isradipine compatibility with different ingredients.

The DSC thermograms for the lyophilized formulation showed an exothermic peak indicating amorphization of the drug after lyophilization; such results were also reported by Jena *et al.* [36]. Isradipine thermograms confirm the drug's crystalline structure; regardless, DSC thermograms of physical combinations and freeze-dried sample F13 also indicated a prominent endothermic peak. According to studies, peak characteristics for pure drug and formulation do not differ; hence, no drug-excipient interactions were deduced in this study.

Consequently, combining Drug: PLA with Poloxamer-407 produces a better dissolving profile than utilizing the drug separately. In addition, several kinetic governing equations, such as zero-order, first-order, and Higuchi models, are used better to understand drug release mechanisms and fit kinetic models. As a result, pure drug release is governed by Fickian diffusion kinetics, but ISRA-optimized PNs are governed by non-Fickian diffusion kinetics.

The increase in bioavailability explains that the drug's solubility profile and absorption through the gastrointestinal membrane have improved. Furthermore, *in vivo* studies suggest that using adjusted PNs of ISRA enhanced the drug's permeation and absorbing potential substantially, as reflected by the significantly improved pharmacokinetic criterion compared to pure isradipine.

The P-XRD study for lyophilized formulation did not exhibit any peaks at any of the 2θ angles suggesting complete amorphization of the drug. The results of the P-XRD study concur with the results of DSC studies. Significant peaks were seen in the pure drug, confirming a characteristic crystalline nature. Nevertheless, the relatively narrow distinct peak at such angles was minimized in optimized ISRA PNs, indicating an amorphous nature and molecular trapping of the drug in the powder form.

In the SEM, the pure-drug ISRA seems to have a rough surface with crystalline characteristics. At the same time, the freeze-dried formulation indicated that the particles appeared spherical.

As a result, the optimized freeze-dried PNs of ISRA were assessed to attain the stability specifications since the CQAs weren't altered significantly with time, reflecting the formulation's stability characteristics in an accelerated state.

CONCLUSION

The systematic creation of PNs of Isradipine, a new hypertension medication, was carried out in this study employing a quality-by-design strategy to optimize drug bioavailability. During the QbD process, the initial QTPPs and CQAs were found and justified. For preliminary screening of the formulations, the Taguchi screening design was used, and the BBD was used for systematic optimization. The regression equation, as well as the response surface, were investigated. To find the effective model term, an ANOVA investigation was performed. The maximum and lower limits of distinct CQAs were established to optimize freeze-dried PNs of Isradipine. The optimum combination for freeze-dried PNs employing BBD was 5 mg ISRA: 5 mg PLA: Poloxamer-407 (1.0% w/v). The improved freeze-dried polymeric nanoparticle samples exhibited an *in vitro* drug release rate of more than 90% at 24h, a particle size of 153.14 nm, and a zeta potential of -25.9 mV, with an entrapment efficiency of 78.25%. Compared to an aqueous suspension of pure medication, *in vivo* studies indicated a 3-fold improvement in oral bioavailability with improved C_{max} and AUC for optimal formulation. The CQAs showed no significant changes in storage after six months, as evidenced by p-values for all CQAs,

according to an accelerated stability assessment of ISRA's optimized PNs. The current research revealed that for the drug's PLA-based polymeric nanoparticles, an ideal amalgamation of 5 mg ISRA: 5 mg PLA and (1.5%w/v) Poloxamer 407 delivered sustained drug release and improved bioavailability.

ACKNOWLEDGMENT

The authors would like to sincerely acknowledge Central Instrumentation Facility of Roland Institute of Pharmaceutical Sciences, Berhampur and also Central Instrumentation Facility, BIT, Pilani Hyderabad, India, for providing the facility to carry out the characterization analysis of Particle size analysis, SEM, P-XRD, during our research.

LIST OF ABBREVIATIONS

AUC: Area under curve, BBD: Box-behnken design, C_{max} : Maximum concentration, CQAs: Critical quality attributes, EE: Entrapment efficiency, ISRA: Isradipine, PNs: Polymeric nanoparticles, P-XRD: Powder X-ray diffractometry, QTPPs: Quality target product profiles, SEM: Scanning electron microscopy, t_{max} : maximum peak concentration time, UFLC: Ultra-fast liquid chromatography

FUNDING

This research did not receive a specific grant from any funding agencies.

CONFLICT OF INTERESTS

The authors declare no conflict of interest.

AUTHORS CONTRIBUTIONS

Debashish Ghose: Major contributor towards writing and language editing or substantively the final form of the document. Chinam Niranjan Patra and Jammula Sruti: checked grammatical and typographical errors, etc. as per the journal guidelines. All authors have read and approved the manuscript. Suryakanta Swain: Conceptualization, Methodology, Software applications, formal analysis.

REFERENCES

1. Patwekar SL, Baramade MK. Controlled release approach to novel multiparticulate drug delivery system. *Int J Pharm Pharm Sci.* 2012;4:757-63.
2. Bernkop Schnurch A. Nanocarrier systems for oral drug delivery: do we really need them? *Eur J Pharm Sci.* 2013;49(2):272-7. doi: 10.1016/j.ejps.2013.03.008. PMID 23537503.
3. Zhang L, Wang S, Zhang M, Sun J. Nanocarriers for oral drug delivery. *J Drug Target.* 2013;21(6):515-27. doi: 10.3109/1061186X.2013.789033, PMID 23621127.
4. Mohanraj VJ, Chen Y. Nanoparticles-a review. *Trop J Pharm Res.* 2006;5(1):561-73. doi: 10.4314/tjpr.v5i1.14634.
5. Mulla MZ, Rahman MRT, Marcos B, Tiwari B, Pathania S. Poly lactic acid (PLA) nanocomposites: effect of inorganic nanoparticles reinforcement on its performance and food packaging applications. *Molecules.* 2021;26(7):1967. doi: 10.3390/molecules26071967, PMID 33807351.
6. Wang Y, Jiang G, Qiu T, Ding F. Preparation and evaluation of paclitaxel-loaded nanoparticle incorporated with galactose-carrying polymer for hepatocyte targeted delivery. *Drug Dev Ind Pharm.* 2012;38(9):1039-46. doi: 10.3109/03639045.2011.637052, PMID 22124381.
7. Ghose D, Patra CN, Ravi Kumar BVV, Swain S, Jena BR, Choudhury P. QbD-based formulation optimization and characterization of polymeric nanoparticles of cinacalcet hydrochloride with improved biopharmaceutical attributes. *Turk J Pharm Sci.* 2021;18(4):452-64. doi: 10.4274/tjps.galenos.2020.08522. PMID 34496552.
8. Girotra P, Singh SK, Kumar G. Development of zolmitriptan loaded PLGA/poloxamer nanoparticles for migraine using quality by design approach. *Int J Biol Macromol.* 2016;85:92-101. doi: 10.1016/j.ijbiomac.2015.12.069. PMID 26724690.
9. Ahmed S, Gull A, Alam M, Aqil M, Sultana Y. Ultrasonically tailored, chemically engineered and "QbD" enabled fabrication

- of agomelatine nanoemulsion; optimization, characterization, ex-vivo permeation and stability study. *Ultrason Sonochem.* 2018;41:213-26. doi: 10.1016/j.ultsonch.2017.09.042. PMID 29137746.
10. Ramasahayam B, Eedara BB, Kandadi P, Jukanti R, Bandari S. Development of isradipine loaded self-nano emulsifying powders for improved oral delivery: *in vitro* and *in vivo* evaluation. *Drug Dev Ind Pharm.* 2015;41(5):753-63. doi: 10.3109/03639045.2014.900081, PMID 24641324.
 11. Alam T, Khan S, Gaba B, Haider MF, Baboota S, Ali J. Adaptation of quality by design-based development of isradipine nanostructured-lipid carrier and its evaluation for *in vitro* gut permeation and *in vivo* solubilization fate. *J Pharm Sci.* 2018;107(11):2914-26. doi: 10.1016/j.xphs.2018.07.021. PMID 30076853.
 12. Dangre P, Gilhotra R, Dhole S. Formulation and statistical optimization of self-microemulsifying drug delivery system of eprosartan mesylate for improvement of oral bioavailability. *Drug Deliv Transl Res.* 2016;6(5):610-21. doi: 10.1007/s13346-016-0318-7, PMID 27465619.
 13. Bonde GV, Ajmal G, Yadav SK, Mittal P, Singh J, Bakde BV. Assessing the viability of Soluplus® self-assembled nanocolloids for sustained delivery of highly hydrophobic lapatinib (anticancer agent): optimisation and *in vitro* characterisation. *Colloids Surf B Biointerfaces.* 2020;185:110611. doi: 10.1016/j.colsurfb.2019.110611. PMID 31704609.
 14. Park SY, Kang Z, Thapa P, Jin YS, Park JW, Lim HJ. Development of sorafenib loaded nanoparticles to improve oral bioavailability using a quality by design approach. *Int J Pharm.* 2019;566:229-38. doi: 10.1016/j.ijpharm.2019.05.064. PMID 31136778.
 15. Garg NK, Tyagi RK, Singh B, Sharma G, Nirbhavane P, Kushwah V. Nanostructured lipid carrier mediates effective delivery of methotrexate to induce apoptosis of rheumatoid arthritis via NF- κ B and FOXO1. *Int J Pharm.* 2016;499(1-2):301-20. doi: 10.1016/j.ijpharm.2015.12.061. PMID 26768725.
 16. Venugopal V, Kumar KJ, Muralidharan S, Parasuraman S, Raj PV, Kumar KV. Optimization and *in vivo* evaluation of isradipine nanoparticles using Box-Behnken design surface response methodology. *OpenNano.* 2016;1:1-15. doi: 10.1016/j.onano.2016.03.002.
 17. Havanoor SM, Manjunath K, Bhagawati ST, Veerapur VP. Isradipine loaded solid lipid nanoparticles for better treatment of hypertension-preparation, characterization and *in vivo* evaluation. *Int J Biopharm.* 2014;5:218-24.
 18. Krishnamoorthy B, Habibur Rahman SM, Tamil Selvan N, Hari Prasad R, Rajkumar M, Siva Selvakumar M. Design, formulation, *in vitro*, *in vivo*, and pharmacokinetic evaluation of nisoldipine-loaded self-nanoemulsifying drug delivery system. *J Nanopart Res.* 2015;17(1):34. doi: 10.1007/s11051-014-2818-z.
 19. Selvadurai M, Kaur G, Santhi K, Parasuraman S. Pharmacokinetic evaluation of newly developed isradipine sustained release formulation. *Int J Drug Deliv.* 2015;7:126-40.
 20. Kale AA, Patravale VB. Design and evaluation of self-emulsifying drug delivery systems (SEDDS) of nimodipine. *AAPS PharmSciTech.* 2008;9(1):191-6. doi: 10.1208/s12249-008-9037-9, PMID 18446481.
 21. Prisant LM, Elliott WJ. Drug delivery systems for treatment of systemic hypertension. *Clin Pharmacokinet.* 2003;42(11):931-40. doi: 10.2165/00003088-200342110-00001, PMID 12908851.
 22. Javed MN, Kohli K, Amin S. Risk assessment integrated QbD approach for development of optimized bicontinuous mucoadhesive limicubes for oral delivery of rosuvastatin. *AAPS PharmSciTech.* 2018;19(3):1377-91. doi: 10.1208/s12249-018-0951-1, PMID 29388027.
 23. Dong M, Liu L, Zhang S. Nanostructural biomaterials and applications. *J Nanomater.* 2016;2016:1-2. doi: 10.1155/2016/5903201.
 24. Mekjaruskul C, Sripanidkulchai B. Kaempferia parviflora nanosuspension formulation for scalability and improvement of dissolution profiles and intestinal absorption. *AAPS PharmSciTech.* 2020;21(2):52. doi: 10.1208/s12249-019-1588-4, PMID 31900735.
 25. McGregor C, Bines E. The use of high-speed differential scanning calorimetry (Hyper-DSC) in the study of pharmaceutical polymorphs. *Int J Pharm.* 2008;350(1-2):48-52. doi: 10.1016/j.ijpharm.2007.08.015, PMID 17890030.
 26. Arifin DY, Lee LY, Wang CH. Mathematical modeling and simulation of drug release from microspheres: implications to drug delivery systems. *Adv Drug Deliv Rev.* 2006;58(12-13):1274-325. doi: 10.1016/j.addr.2006.09.007. PMID 17097189.
 27. Janga KY, Jukanti R, Velpula A, Sunkavalli S, Bandari S, Kandadi P. Bioavailability enhancement of zaleplon via proliposomes: role of surface charge. *Eur J Pharm Biopharm.* 2012;80(2):347-57. doi: 10.1016/j.ejpb.2011.10.010. PMID 22041602.
 28. Legrand P, Lesieur S, Bochet A, Gref R, Raatjes W, Barratt G. Influence of polymer behaviour in organic solution on the production of polylactide nanoparticles by nanoprecipitation. *Int J Pharm.* 2007;344(1-2):33-43. doi: 10.1016/j.ijpharm.2007.05.054. PMID 17616282.
 29. Ahad A, Aqil M, Kohli K, Sultana Y, Mujeeb M, Ali A. Formulation and optimization of nanotransfersomes using experimental design technique for accentuated transdermal delivery of valsartan. *Nanomedicine.* 2012;8(2):237-49. doi: 10.1016/j.nano.2011.06.004. PMID 21704600.
 30. Lacourciere Y, Poirier L, Dion D, Provencher P. Antihypertensive effect of isradipine administered once or twice daily on ambulatory blood pressure. *Am J Cardiol.* 1990;65(7):467-72. doi: 10.1016/0002-9149(90)90812-f, PMID 2137666.
 31. Reddy DV, RAO AS. Preparation and evaluation of nanosponges based tramadol HCl c/r tablets using design of experiment. *Int J App Pharm.* 2022;14(3):86-94. doi: 10.22159/ijap.2022v14i3.44278.
 32. Kakade P, Gite S, Patravale V. Development of atovaquone nanosuspension: quality by design approach. *Curr Drug Deliv.* 2020;17(2):112-25. doi: 10.2174/1567201817666191227095019, PMID 31880260.
 33. Te Boekhorst BC, Jensen LB, Colombo S, Varkouhi AK, Schiffelers RM, Lammers T. MRI-assessed therapeutic effects of locally administered PLGA nanoparticles loaded with anti-inflammatory siRNA in a murine arthritis model. *J Control Release.* 2012;161(3):772-80. doi: 10.1016/j.jconrel.2012.05.004. PMID 22580113.
 34. Deka T, Das MK, Das S, Das P, Singha LR. Box-behnken design approach to develop nano-vesicular herbal gel for the management of skin cancer in experimental animal model. *Int J App Pharm.* 2022;14(6):148-66. doi: 10.22159/ijap.2022v14i6.45867.
 35. Shelar DB, Pawar SK, Vavia PR. Fabrication of isradipine nanosuspension by anti-solvent microprecipitation-high-pressure homogenization method for enhancing dissolution rate and oral bioavailability. *Drug Deliv Transl Res.* 2013;3(5):384-91. doi: 10.1007/s13346-012-0081-3, PMID 25788346.
 36. Jena GK, Patra CN, Panigrahi KC, Sruti J, Patra P, Parhi R. QbD enabled optimization of solvent shifting method for fabrication of PLGA-based nanoparticles for promising delivery of capecitabine for antitumor activity. *Drug Deliv Transl Res.* 2022;12(6):1521-39. doi: 10.1007/s13346-021-01042-0, PMID 34505271.